

FORTSCHRITT-
98 ERICHTE
A
3915

VDI

Dipl.-Ing. Stefan Kaiser, München

**Multi-Carrier CDMA
Mobile Radio Systems -
Analysis and Optimization
of Detection, Decoding,
and Channel Estimation**

Reihe **10**: Informatik/
Kommunikationstechnik Nr. **531**

Contents

1	Introduction	1
1.1	Progress in Wireless Communications	1
1.2	Multi-Carrier CDMA for Mobile Communications	4
1.2.1	Principles of DS Spread Spectrum and Multi-Carrier Modulation	4
1.2.2	CDMA Concepts with Multi-Carrier Modulation	6
1.2.3	State of the Art in the Field of MC-CDMA	10
1.3	Goals of the Thesis	13
1.4	Contents and Important Results	14
2	Mobile Radio Channel	16
2.1	Time-Variant Multipath Propagation	16
2.2	Channel Models for Macro-, Micro-, and Picocells	22
2.2.1	CODIT and COST 207 Channel Models	22
2.2.2	Uncorrelated Fading Channel Model for Multi-Carrier Systems	29
3	Multiple Access Scheme MC-CDMA	31
3.1	Multi-Carrier Communications	31
3.1.1	Orthogonal Frequency Division Multiplexing	31
3.1.2	Principle of MC-FDMA, MC-TDMA, and MC-CDMA	38
3.2	MC-CDMA Signal Structure	38
3.3	MC-CDMA Data Detection Techniques	46
3.3.1	Introduction	46
3.3.2	Single-User Detection	49
3.3.3	Interference Cancellation	53
3.3.4	Joint Detection with Maximum Likelihood Criterion	54
3.4	Performance of Uncoded MC-CDMA Systems	56
3.5	Equivalence between MC-CDMA and DS-CDMA	62

MC-CDMA systems with soft decision decoding applying SD as well as MD have to be derived. The iterative concatenation of data detection and decoding for IC with reliability information shall be investigated. The trade-off between coding and spreading in MC-CDMA mobile radio systems shall be found.

- A powerful channel estimation concept is required for MC-CDMA systems to guarantee efficient coherent data detection and soft decision channel decoding. Channel estimation concepts with filtering in two dimensions shall be developed and analyzed generally for MC modulated systems operating in mobile radio channels with fast time variation and large time dispersion, typical for large cells.
- Future cellular mobile radio systems have to operate in hierarchical cell structures with cells of various size, adapted to the specific environment and requirement. Three typical cell classifications can be distinguished, macro-, micro-, and picocells, where each class has its characteristic signal propagation. To the best of the author's knowledge, no complete system analysis of a coded MC-CDMA mobile radio system with non-perfect channel estimation for all three propagation scenarios typical for future cellular concepts is available. An extensive system analysis of an MC-CDMA system in the downlink with channel coding and non-perfect channel estimation shall be carried out for mobile radio channels, typical for macro-, micro-, and picocell propagation scenarios. This analysis shall prove the suitability of an MC-CDMA system as a potential candidate for future mobile radio systems.

1.4 Contents and Important Results

The thesis consists of 7 chapters, where the contents of the Chapters 3 to 6 correspond to the goals mentioned in Section 1.3.

The fundamentals of time variant multipath propagation, which characterize the demands on a mobile radio system, are summarized in Chapter 2. After describing the mobile radio channel and its statistical modelling, channel models typical for future cellular mobile radio systems are classified for macro-, micro-, and picocells.

In Chapter 3, the MC-CDMA concept under investigation is presented. After an introduction into MC modulation with OFDM, the MC-CDMA signal structure is explained and its flexibility is pointed out by introducing the M -, the Q -, and the $M&Q$ -Modification. A discrete-time and -frequency MC-CDMA transmission model is mathematically described using the vector-matrix notation. Low-complex SD techniques, a multistage detection technique with IC, where the detection stages are adapted to the residual MAI, and the optimum JD with MLSSE are developed and analyzed for MC-CDMA systems. Their performance is demonstrated and compared to known SD and MD techniques based on Monte Carlo simulations. The principle of MC-FDMA and MC-TDMA is briefly introduced and the performance of MC-CDMA, MC-FDMA, and MC-TDMA systems is compared to each other. Finally, the equivalence between MC-CDMA and DS-CDMA is pointed out in Chapter 3.

According to OFDM, the N_c substreams are modulated on subcarriers with a spacing of

$$F_s = \frac{1}{T_s} \quad (3.2)$$

to achieve orthogonality between the signals on the N_c subcarriers, presuming a rectangular pulse shaping. The N_c parallel modulated source symbols S_n , $n = 1, \dots, N_c$, are referred to as an OFDM symbol of duration T_s . The complex envelope of an OFDM symbol with rectangular pulse shaping has the form

$$x(t) = \frac{1}{\sqrt{N_c}} \sum_{n=1}^{N_c} S_n \operatorname{rect}\left(\frac{t}{T_s} - \frac{1}{2}\right) e^{j2\pi f_n t}. \quad (3.3)$$

In (3.3), the factor $1/\sqrt{N_c}$ normalizes the energy. The N_c subcarrier frequencies are located at

$$f_n = \frac{n-1}{T_s}, \quad n = 1, \dots, N_c, \quad (3.4)$$

where the center of the frequency spectrum is located at $(N_c - 1)/(2T_s)$. This definition of f_n , $n = 1, \dots, N_c$, facilitates a simple mathematical modelling. The carrier frequency f_c determining the location of the signal in the bandpass domain is neglected in (3.4), since the equivalent lowpass domain is considered. The energy density spectrum $|X(f)|^2$ of an OFDM symbol is the sum of the energy density spectra of N_c independently modulated subcarriers and results in

$$|X(f)|^2 = \frac{1}{N_c} \sum_{n=1}^{N_c} \left| S_n T_s \frac{\sin(\pi(f - f_n)T_s)}{\pi(f - f_n)T_s} \right|^2. \quad (3.5)$$

The normalized energy density spectrum of an OFDM symbol with N_c equal to 16 subcarriers versus the normalized frequency fT is depicted as a solid curve in Fig. 3.1. The OFDM spectrum is shown for the case where the symbols S_n , $n = 1, \dots, N_c$, are transmitted with equal energy. The dotted curve illustrates the energy density spectrum of the first modulated subcarrier f_1 and indicates the construction of the overall energy density spectrum as the sum of N_c , each by $1/T_s$ shifted, individual energy density spectra. For large values of $fT \in [-0.5, 0.5]$ containing the subcarriers. Only subcarriers near the band edges contribute to the out-of-band power. Therefore, as N_c becomes large, the energy density spectrum approaches that of single carrier modulation with ideal Nyquist filtering. As a reference, the normalized energy density spectrum of binary phase shift keying (BPSK) [Pro95] is plotted as a dashed curve.

A key advantage of using OFDM is that the MC modulation can be implemented in the discrete domain by using an IDFT, or a more computationally efficient IFFT [WeE71]. When sampling the complex envelope $x(t)$ of an OFDM symbol at time instances t equal to $(\nu - 1)T_s/N_c$, $\nu = 1, \dots, N_c$, the samples are

$$x_\nu = \frac{1}{\sqrt{N_c}} \sum_{n=1}^{N_c} S_n e^{j2\pi(n-1)(\nu-1)/N_c}, \quad \nu = 1, \dots, N_c, \quad (3.6)$$

and the sampling rate is N_c/T_s . The important result is that the sampled sequence $\{x_\nu\}$, $\nu = 1, \dots, N_c$, is the IDFT of the source symbol sequence $\{S_n\}$, $n = 1, \dots, N_c$. The block

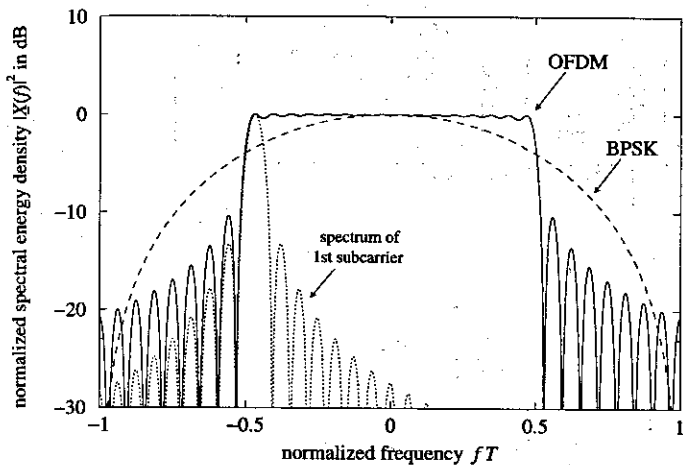


Figure 3.1: Normalized energy density spectrum versus normalized frequency fT of an OFDM symbol with $N_c = 16$ subcarriers, of the first subcarrier, and of BPSK

diagram of an MC modulator employing OFDM based on an IDFT and MC demodulator employing inverse OFDM based on a DFT is illustrated in Fig. 3.2.

When the number of subcarriers increases, the OFDM symbol duration T_s becomes large compared to the duration of the impulse response τ_{\max} of the channel and the amount of ISI reduces. However, to completely avoid the effect of ISI and, thus, to maintain the orthogonality between the signals on the N_c subcarriers, i.e., also to avoid ICI, a guard interval of duration

$$T_g \geq \tau_{\max} \quad (3.7)$$

has to be inserted between adjacent OFDM symbols [AIL87, Bin90, Pro95]. The guard interval is a cyclic prefix added to each OFDM symbol which is obtained by extending the duration of an OFDM symbol to

$$T'_s = T_g + T_s. \quad (3.8)$$

The discrete length of the guard interval has to be

$$L_g \geq \left\lceil \frac{\tau_{\max} N_c}{T_s} \right\rceil \quad (3.9)$$

samples to prevent ISI. The sampled sequence $\{x_\nu\}$ with cyclic extended guard interval results in

$$x_\nu = \frac{1}{\sqrt{N_c}} \sum_{n=1}^{N_c} S_n e^{j2\pi(n-1)(\nu-1)/N_c}, \quad \nu = 1 - L_g, \dots, N_c. \quad (3.10)$$

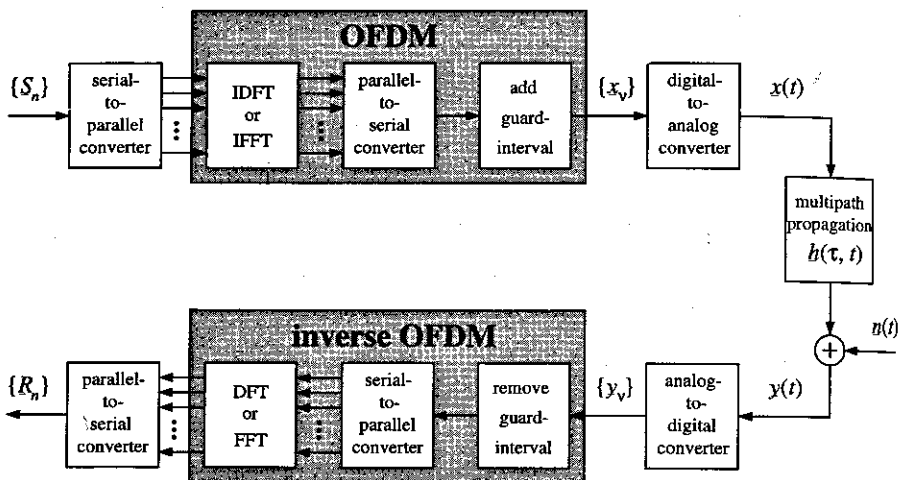


Figure 3.2: MC transmission system with OFDM

In practice, the sampled sequence $\{x_\nu\}$, $\nu = 1 - L_g, \dots, N_c$, is passed through a digital-to-analog converter whose output ideally would be the signal waveform $x(t)$ given in (3.3) with increased duration T_s' .

The output of the channel is the signal waveform $y(t)$ obtained from convolution of $x(t)$ with the channel impulse response $h(\tau, t)$ and addition of a noise signal $n(t)$, i.e.,

$$y(t) = \int_0^{T_{\max}} x(t - \tau) h(\tau, t) d\tau + n(t). \quad (3.11)$$

The noise signal $n(t)$ contains the inherent disturbances of the transmission system, which are, motivated by the central limit theorem, modelled as additive white Gaussian noise (AWGN). The received signal $y(t)$ is passed through an analog-to-digital converter, whose output sequence $\{y_\nu\}$, $\nu = 1 - L_g, \dots, N_c$, is the received signal $y(t)$ sampled at rate N_c/T_s . Since ISI is only present in the first L_g samples of the received sequence, these L_g samples are removed before MC demodulation. The ISI-free part $\nu = 1, \dots, N_c$ of $\{y_\nu\}$ is MC demodulated by inverse OFDM exploiting a DFT. The output of the DFT is the MC demodulated sequence $\{B_n\}$, $n = 1, \dots, N_c$, consisting of N_c complex-valued symbols

$$B_n = \frac{1}{\sqrt{N_c}} \sum_{\nu=1}^{N_c} y_\nu e^{-j2\pi(n-1)(\nu-1)/N_c}, \quad n = 1, \dots, N_c. \quad (3.12)$$

Since ICI can be avoided due to the guard interval, each subchannel can be considered separately. When, furthermore, assuming that the fading on each subchannel is flat and ISI is

Appendix B

Multiple Access Scheme SS-MC-MA

B.1 SS-MC-MA Signal Structure

This section presents a novel multiple access scheme which is referred to as spread spectrum multi-carrier multiple access (SS-MC-MA). Similar to MC-CDMA, SS-MC-MA exploits the advantages given by the combination of the spread spectrum technique with MC modulation [KaF96, KaF97a]. An SS-MC-MA system is superior compared to an MC-CDMA system in the uplink of a mobile radio system due to a simple channel estimation and a low-complex data detection. Whereas, an MC-CDMA system outperforms an SS-MC-MA system in the downlink, as it will be shown at the end of this section. Before presenting the SS-MC-MA signal structure and its uplink performance, the basic similarities and differences between SS-MC-MA and MC-CDMA systems are pointed out. This can preferably be done by comparing the SS-MC-MA and the MC-CDMA transmitter for the downlink. Fig. B.1 shows the SS-MC-MA transmitter for the downlink. The counterpart is the MC-CDMA transmitter with M -Modification shown

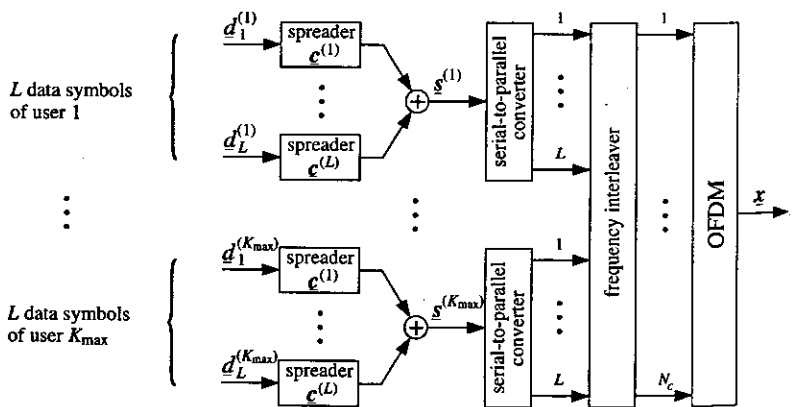


Figure B.1: Principle of SS-MC-MA illustrated for the transmitter in the downlink to enable a comparison with MC-CDMA shown in Fig. 3.8

in Fig. 3.8. For convenience, the case with M equal to L and K_{\max} equal to L is considered in this comparison. It can be observed that both transmitters are identical except for the mapping of the user data to the subsystems. In SS-MC-MA systems, one user maps L data symbols to one subsystem which this user exclusively uses for transmission. Consequently, different users use different subsystems in SS-MC-MA systems. In MC-CDMA systems, M data symbols per user are mapped to M different subsystems where each subsystem is shared by different users.

Between SS-MC-MA and MC-CDMA systems exist the following similarities:

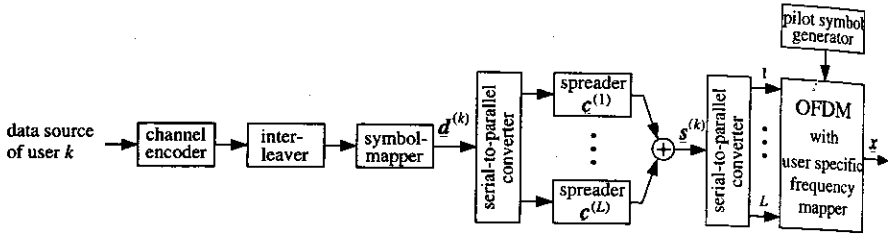
- SS-MC-MA and MC-CDMA systems exploit frequency diversity by spreading each data symbol over L subcarriers.
- Per subsystem, the same data detection techniques can be applied with both SS-MC-MA and MC-CDMA systems.
- ISI and ICI can be avoided in SS-MC-MA and MC-CDMA systems, resulting in simple data detection techniques.

Between SS-MC-MA and MC-CDMA systems exist the following differences:

- In SS-MC-MA systems, the code division is used for the simultaneous transmission of the data of one user on the same subcarriers, whereas in the case of MC-CDMA systems, the code division is used for the transmission of the data of different users on the same subcarriers. Therefore, SS-MC-MA is an FDMA scheme on subcarrier level, whereas MC-CDMA is a CDMA scheme.
- MC-CDMA systems have to cope with MAI, which is not present in SS-MC-MA systems. Instead of MAI, the SS-MC-MA system has to cope with self interference caused by the superposition of signals from the same user.
- In SS-MC-MA systems, each subcarrier is exclusively used by one user, enabling low complex channel estimation especially for the uplink. In MC-CDMA systems, the channel estimation in the uplink has to cope with the superposition of signals from different users which are faded independently on the same subcarriers, increasing significantly the complexity of the uplink channel estimation.
- In an MC-CDMA system, M data symbols are spread over $M \cdot L$ subcarriers, whereas in an SS-MC-MA system, L data symbols are spread over the same L subcarriers. Hence, MC-CDMA is able to exploit more frequency diversity.

After this comparative introduction of SS-MC-MA, the uplink transmitter and the assigned receiver are described in detail in the sequel.

SS-MC-MA Transmitter: Fig. B.2 shows an SS-MC-MA transmitter with channel coding for the data of the k th user, $k = 1 \dots K$, for the uplink. The components channel encoding,

Figure B.2: SS-MC-MA transmitter of the k th user for the uplink

interleaving, and symbol mapping are identical to those described in Chapter 4 for MC-CDMA systems. In SS-MC-MA systems, L subsequent complex-valued data symbols $d_l^{(k)}$, $l = 1 \dots L$, of user k are serial-to-parallel converted. The vector

$$\mathbf{d}^{(k)} = (d_1^{(k)}, d_2^{(k)}, \dots, d_L^{(k)})^T \quad (\text{B.1})$$

represents one block of L parallel converted data symbols of the k th user. Each of the L data symbols is multiplied with another orthogonal spreading code of length L . The $L \times L$ matrix

$$\mathbf{C} = (\mathbf{c}_1 \ \mathbf{c}_2 \ \dots \ \mathbf{c}_L) = \begin{pmatrix} C_{1,1} & C_{2,1} & \dots & C_{L,1} \\ C_{1,2} & C_{2,2} & \dots & C_{L,2} \\ \vdots & & \ddots & \vdots \\ C_{1,L} & C_{2,L} & \dots & C_{L,L} \end{pmatrix} \quad (\text{B.2})$$

represents the L different spreading codes \mathbf{c}_l , $l = 1, \dots, L$, used by user k . The matrix \mathbf{C} is the same for all users. The modulated spreading codes are data symbol and, thus, chip synchronously added, resulting in the transmission vector

$$\mathbf{s}^{(k)} = \mathbf{C} \mathbf{d}^{(k)} = (S_1^{(k)}, S_2^{(k)}, \dots, S_L^{(k)})^T \quad (\text{B.3})$$

consisting of L components. To increase the robustness of SS-MC-MA systems e.g. against inter cell interference, less than L data modulated spreading codes can be added to one transmission vector $\mathbf{s}^{(k)}$.

Comparable to the frequency interleaving in MC-CDMA systems, the SS-MC-MA transmitter performs a user specific frequency mapping [KaF97b] such that subsequent components of $\mathbf{s}^{(k)}$ are interleaved and mapped to subcarriers with maximum distance. The subcarriers of the different subsystems are chosen such that each subsystem exploits the whole transmission bandwidth. The user specific frequency mapping assigns each subsystem and, hence, each user exclusively its L subcarriers, avoiding MAI. The Q -Modification introduced in Section 3.2 for MC-CDMA systems is inherent in SS-MC-MA systems. The M -Modification can similar as for MC-CDMA systems be applied to SS-MC-MA systems by assigning a user more than one subsystem.

OFDM with guard interval is applied in SS-MC-MA systems in the same way as in MC-CDMA systems, cf. Section 3.1.1. In order to perform coherent data detection at the receiver and to guarantee robust time and frequency synchronization, pilot symbols are multiplexed in the transmitted data.

SS-MC-MA Receiver: An SS-MC-MA receiver with coherent detection of the data of the k th user is shown in Fig. B.3. After inverse OFDM with user specific frequency demapping and

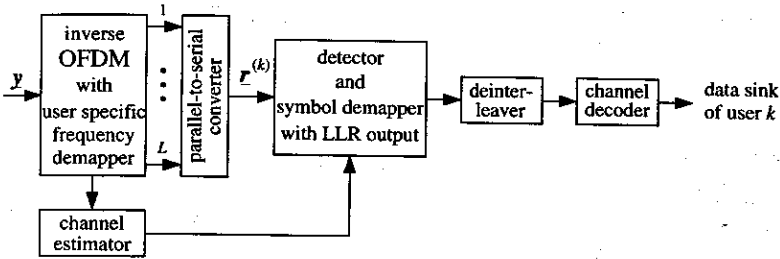


Figure B.3: SS-MC-MA receiver of the k th user

extraction of the pilot symbols from the symbols with user data, the MC demodulated vector

$$\mathbf{r}^{(k)} = \mathbf{H}^{(k)} \mathbf{s}^{(k)} + \mathbf{v}^{(k)} = (R_1^{(k)}, R_2^{(k)}, \dots, R_L^{(k)})^T \quad (\text{B.4})$$

with the data of the k th user is obtained, where the $L \times L$ diagonal matrix $\mathbf{H}^{(k)}$ and the vector $\mathbf{v}^{(k)}$ of length L describe the channel fading and noise, respectively, on the subcarriers exclusively used by the k th user.

Any of the SD or MD data detection techniques presented for MC-CDMA systems in Section 3.3 can be applied for the detection of the data of a single user per subsystem in SS-MC-MA systems. However, SS-MC-MA systems offer especially in the downlink the advantage that with JD in one estimation step simultaneously L data symbols of a single user are estimated. Compared to MC-CDMA systems, the complexity of JD per data symbol in SS-MC-MA systems reduces by a factor of L in the downlink. With JD, LLRs can inherently be obtained from the detection algorithm which may also include the symbol demapping, cf. Chapter 4. After deinterleaving and decoding of the LLRs, the detected source bits of the k th user are obtained.

B.2 Performance

In the following, the performance of an SS-MC-MA mobile radio system in the uplink is presented. Table B.1 shows the SS-MC-MA system parameters used in the uplink. These parameters are chosen such that they correspond as far as possible with the MC-CDMA system

Table B.1: Basic parameters of the proposed SS-MC-MA mobile radio system

bandwidth	$B = 2 \text{ MHz}$
carrier frequency	$f_c = 1.8 \text{ GHz}$
TDMA frame duration	$T_{\text{TDMA}} = 18.4 \text{ ms}$
number of OFDM frames per TDMA frame	$N_{\text{fr}} = 4$
OFDM frame duration	$T_{\text{fr}} = 4.6 \text{ ms}$
number of OFDM symbols per OFDM frame	$N_s = 31$
OFDM, inverse OFDM	256 point IFFT, 256 point FFT
OFDM symbol duration including guard interval	$T'_s = 148 \mu\text{s}$
guard interval duration	$T_g = 20 \mu\text{s}$
subcarrier spacing	$F_s = 7.8 \text{ kHz}$
total number of subcarriers used per user	$N'_c = 8$
spreading code	Walsh Hadamard code
spreading code length	$L = 8$
data detector	MLSSE
data symbol mapping	QPSK with Gray encoding
channel code	convolutional code
code rate	$R = 1/2$
memory	$M_c = 6$
channel decoder	Viterbi decoder
code bit interleaver	pseudo random interleaver
code bit interleaver size	$I_c = 384$
channel estimator	1-D FIR filters
filter taps	$N_{\text{tap}} = 5$
Doppler filter bandwidth	$f_{D,\text{filter}} = 333.3 \text{ Hz}$
pilot symbol distance in time	$N_t = 5$
maximum number of active users per OFDM frame	$K_{\text{max}} = 32$
user capacity	$K_{\text{sys}} = 128$
net bit rate per user	$10.5 \text{ kbit/s} \leq R_b \leq 1.3 \text{ Mbit/s}$
bandwidth efficiency	$\beta = 0.67 \text{ bit/s/Hz}$

parameters for the downlink presented in Table 6.1. The SS-MC-MA system parameters described in the following differ from those of the MC-CDMA system presented in Chapter 6. The SS-MC-MA system transmits only on 256 subcarriers. Since the channel estimation in the considered SS-MC-MA system is based on a 1-D filtering in time direction which should fulfill two-times oversampling of the time-variant fading process, the overhead due to pilot symbols

can be reduced with decreasing OFDM symbol durations. However, it has to be taken into account that with decreasing OFDM symbol duration the loss in bandwidth efficiency due to the guard interval increases. The used TDMA frame structure consisting of 4 time slots. A time slot corresponds to an OFDM frame consisting of 31 OFDM symbols as illustrated in Fig. B.4. Each user exclusively transmits on 8 subcarriers, where 3 of the 8 subcarriers used by

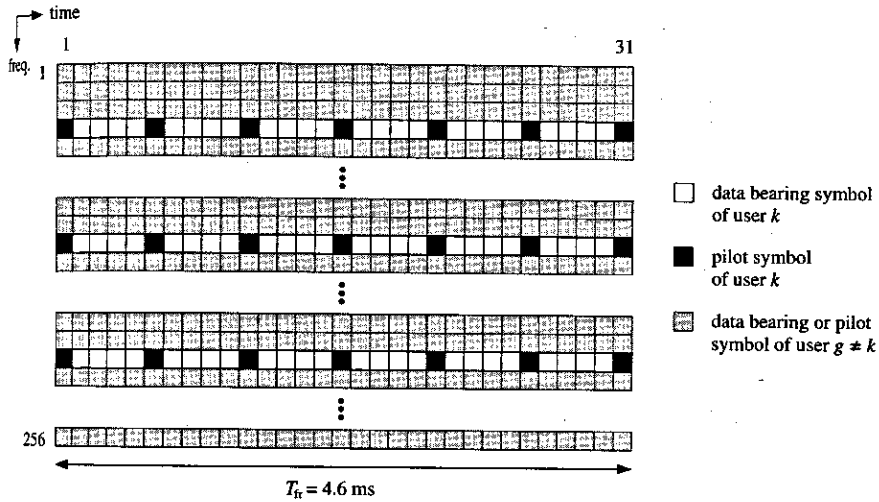


Figure B.4: OFDM frame of the proposed SS-MC-MA mobile radio system; $N_c = 256$; $N_s = 31$; $N_t = 5$; $N_{grid} = 1792$

the k th user are depicted. Hence, per user, a block of 8 serial data symbols is parallel converted and spread with orthogonal Walsh Hadamard codes of length L equal to 8, resulting after superposition in the transmission sequence $g^{(k)}$, cf. (B.3). Note that in contrast to Fig. B.2, an additional interleaver is applied which scrambles 192 components of 24 transmission sequences $f^{(k)}$ with the intention to increase the diversity potential of the system. Per OFDM symbol, 8 randomly interleaved components are mapped on 8 subcarriers exclusively used by the k th user. The 8 user specific subcarriers are distributed over the whole bandwidth. The receiver applies an MLSSE for data detection. The channel coding part is identical to that of the MC-CDMA system presented in Chapter 6.

For the uplink channel estimation, a simple 1-D filtering in time direction is used per subcarrier. The 1-D FIR filter is designed as 1-D Wiener filter for a rectangular Doppler power spectrum where $f_{D,filter} = 333.3$ Hz is chosen as worst case condition. The pilot symbol spacing in time direction N_t is chosen equal to 5 to two-times oversample the dynamics of the fading in time direction, given $f_{D,max} = 333.3$ Hz. The 1-D FIR filter is realized with 5 taps, which is a good compromise between performance and complexity [HKR97a].

The average coded BER P_b versus the SNR γ_b for the presented SS-MC-MA system in the uplink is shown in Fig. B.5. The COST 207 channel models, each with different velocities v of the MS, are considered. It should be noted that the performance of the SS-MC-MA system is independent of the number of active users due to the avoidance of MAI, i.e., the presented performance is valid for a fully loaded system and also for a system with only one active user. The total SNR loss due to the guard interval and the pilot symbols is 1.6 dB and is taken into

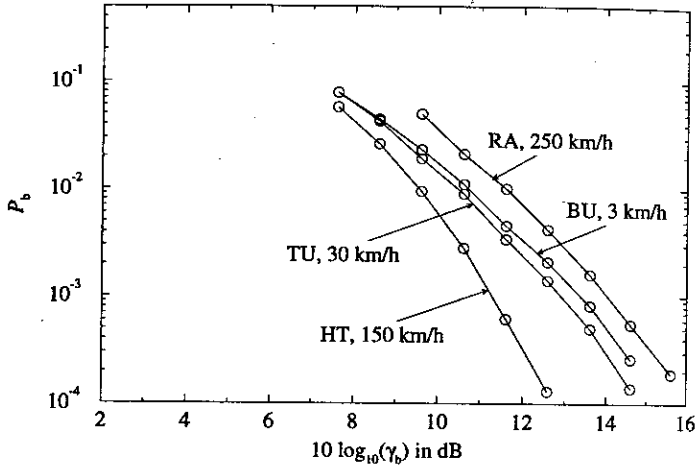


Figure B.5: Average coded BER P_b versus average SNR γ_b per bit for the SS-MC-MA system in the uplink; COST 207 channel models: different velocities v of the MS; MLSSE; 1-D channel estimation; $L = 8$; QPSK; $R = 1/2$

account in the results of Fig. B.5. It can be observed that even in a scenario with velocity of 250 km/h in a rural area, an SNR of 14 dB is sufficient to guarantee a BER P_b less than 10^{-3} . The proposed SS-MC-MA system achieves for the uplink the bandwidth efficiency of

$$\beta = 0.67 \text{ bit/s/Hz.} \quad (\text{B.5})$$

In the downlink, an SS-MC-MA system can achieve the same high bandwidth efficiency as the MC-CDMA system presented in Chapter 6, when also applying channel estimation in two dimensions. To fair compare the performance of the MC-CDMA system proposed in Chapter 6 with the performance of the SS-MC-MA system proposed in this section, the influence due to the different channel estimation concepts is avoided by comparing the performance under the assumption of perfect channel estimation. In Table B.2, the SNR γ_b degradation of the SS-MC-MA system compared to the MC-CDMA system is given for the four propagation scenarios under investigation at a BER P_b of 10^{-3} . The MC-CDMA system shows a significant performance improvement compared to the SS-MC-MA system in the propagation scenario BU,

Table B.2: SNR degradation of the presented SS-MC-MA mobile radio system compared to the MC-CDMA mobile radio system investigated in Chapter 6; perfect channel estimation

	BU	TU	HT	RA
	$v=3$ km/h	$v=30$ km/h	$v=150$ km/h	$v=250$ km/h
SNR degradation in dB	1.6	0.8	1.0	1.1

v equal to 3 km/h, which has less time diversity. As already mentioned, MC-CDMA systems can better exploit frequency diversity compared to SS-MC-MA systems. If the propagation scenario offers time diversity, the SNR degradation with the SS-MC-MA system compared to the MC-CDMA system is about 1 dB. For more details about the performance and flexibility of SS-MC-MA mobile radio systems, the reader is referred to [KaF97a, KaF97b].

It can be concluded that a promising future mobile radio system may use in the downlink the MC-CDMA system proposed in Chapter 6, and in the uplink the SS-MC-MA system proposed in this section. This combination achieves for both links a high bandwidth efficiency and great flexibility. Furthermore, in both links the same hardware can be used, only the user data have to be mapped differently.

L_b	length of the code bit vector $\mathbf{b}^{(k)}$
L_d	length of the data symbol vector $\mathbf{d}^{(k)}$
L_g	length of guard interval
$\mathcal{L}^{(k)}$	log-likelihood ratio assigned to $b^{(k)}$
$\mathcal{L}_{re}^{(q)[j]}$	log-likelihood ratio ratios after re-encoding for soft IC, j th iteration
$\mathcal{L}_x^{(k)}$	log-likelihood ratio assigned to $b_x^{(k)}$
m	parameter of the Nakagami- m distribution
m_p	parameter of the Nakagami- m distribution assigned to the p th path
M	number of data symbols transmitted per user and OFDM symbol
M_c	memory of channel code
M_d	maximum number of different realizations of a data symbol $\mathbf{d}^{(k)}$
M_s	maximum number of different realizations of a chip $C_i^{(k)}$
$\mathbf{n}(t)$	additive noise signal
\mathbf{n}	noise vector
N_c	number of subcarriers
N_l	l th element of the noise vector \mathbf{n}
N_f	pilot symbol distance in frequency direction
N_{fr}	number of time slots per TDMA frame
N_{grid}	number pilot symbols per OFDM frame
N_p	number of path
N_s	number of OFDM symbols per OFDM frame
N_t	pilot symbol distance in time direction
N_{tap}	number of filter taps
N_w	number of waves assigned to one scatterer
$p(\cdot)$	probability density function
$P\{\cdot\}$	probability
P_b	average BER
\mathcal{P}	set of pilot positions in an OFDM frame
Q	number of user groups
$Q\{\cdot\}$	quantization operation
\mathbf{r}	received vector after inverse OFDM
$\mathbf{r}^{(k)}$	received vector of the k th user after inverse OFDM
R	code rate
$B(\tau_1, \tau_2, \Delta t)$	autocorrelation function of a WSS channel impulse response
R_b	bit rate
R_l	l th element of the received vector \mathbf{r}
\mathbf{s}	source vector before OFDM
$\mathbf{s}^{(k)}$	source vector of the k th user before OFDM
\mathbf{s}_m	source vector containing the m th transmitted data symbol before OFDM
\mathbf{s}_q	source vector of the q th user group before OFDM
$S(\tau, f_D)$	scattering function

- [Vit95] A. J. Viterbi, *CDMA Principles of Spread Spectrum Communication*. Reading: Addison-Wesley, 1995.
- [WeE71] S. B. Weinstein and P. M. Ebert, "Data transmission by frequency-division multiplexing using the discrete Fourier transform," *IEEE Transactions on Communication Technology*, vol. 19, pp. 628-634, Oct. 1971.
- [YeL94a] N. Yee and J.-P. Linnarz, "Controlled equalization of multi-carrier CDMA in an indoor Rician fading channel," in *Proceedings IEEE Vehicular Technology Conference (VTC'94)*, Stockholm, Sweden, pp. 1665-1669, June 1994.
- [YeL94b] N. Yee and J.-P. Linnarz, "Wiener filtering of multi-carrier CDMA in Rayleigh fading channel," in *Proceedings IEEE International Symposium on Personal, Indoor and Mobile Radio Communications (PIMRC'94)*, The Hague, The Netherlands, pp. 1344-1347, Sept. 1994.
- [YLF93] N. Yee, J.-P. Linnarz, and G. Fettweis, "Multi-carrier CDMA in indoor wireless radio networks," in *Proceedings IEEE International Symposium on Personal, Indoor and Mobile Radio Communications (PIMRC'93)*, Yokohama, Japan, pp. 109-113, Sept. 1993.